Imaging Science in Dentistry 2025; 55: 48-55
https://doi.org/10.5624/isd.20240214

Effect of milliamperage on cone-beam computed tomography evaluation of bone grafts around dental implants

Henrique Mateus Alves Felizardo[1], Bruna Silveira Troca[1], Polyane Mazucatto Queiroz[2], Hugo Gaêta-Araujo[3,*]

[1]*School of Dentistry, Federal University of Alfenas, Alfenas, Minas Gerais, Brazil*
[2]*Department of Dentistry, Ingá Center University, Maringá, Paraná, Brazil*
[3]*Department of Stomatology, Public Health and Forensic Dentistry, Ribeirao Preto School of Dentistry, University of Sao Paulo, Ribeirao Preto, Sao Paulo, Brazil*

ABSTRACT

Purpose: Bone grafts can be challenging to assess on cone-beam computed tomography (CBCT) examinations due to their discreet appearance and the potential introduction of metallic artifacts from implant screws. This study aimed to evaluate the effect of CBCT milliamperage (mA) on detecting bone graft dehiscence adjacent to titanium (Ti) and zirconia (Zr) implants.

Materials and Methods: Twenty Ti and 20 Zr implants were installed in bovine rib blocks. Gaps of at least 2 mm were created between the implant and the bone and filled with particulate autogenous bone grafts. In half of the blocks, the gap was completely filled, while in the other half, the grafting material was removed up to the third implant thread. CBCT images were acquired at 4, 6.3, and 10 mA and evaluated by 5 observers to detect bone graft dehiscence. The area under the receiver operating characteristic curve, accuracy, sensitivity, and specificity were calculated. These values were then compared across various dental implant materials and mA levels using 2-way analysis of variance with a significance level of 5%.

Results: No statistically significant differences were observed in the diagnostic values for bone graft dehiscence between implant types ($P>0.05$) or mA settings ($P>0.05$).

Conclusion: Although a protocol with lower radiation exposure (that is, lower mA) could be employed, the use of CBCT for evaluating bone graft dehiscence adjacent to different types of dental implants should be approached with caution. ***(Imaging Sci Dent 2025; 55: 48-55)***

KEY WORDS: Radiology; Cone-Beam Computed Tomography; Dental Implants; Autografts

Introduction

Installing a dental implant immediately after tooth extraction significantly reduces the number of surgical interventions and treatment time.[1,2] With a success rate of about 98% after 1 year, this procedure is highly effective.[2] However, immediate implant placement poses a risk of bone tissue loss and reduction in bone crest size.[3,4] For minimizing peri-implant bone resorption and maintaining bone structure, autogenous grafts are considered the optimal solution due to their capacity to promote bone growth and establish an immunological bone structure akin to the recipient bed.[5] Therefore, for superior hard tissue preservation, the use of bone grafts during immediate implant placement in alveolar spaces is highly recommended.[6]

In the absence of clinical concerns or symptoms, periapical radiographs are frequently used as the imaging modality of choice for the postoperative assessment of dental implants.[7,8] However, due to their 2-dimensional nature,

This study was supported in part by Coordenação de Aperfeiçoamento de Pessoal de Nível Superior (CAPES - Finance Code 001) and NEODENT (Research 22.0525).
Received October 23, 2024; Revised December 21, 2024; Accepted December 24, 2024
Published online March 10, 2025
*Correspondence to : Prof. Hugo Gaêta-Araujo
Department of Stomatology, Public Health and Forensic Dentistry, Ribeirao Preto School of Dentistry, University of Sao Paulo, Av. do Cafe S/N, Ribeirao Preto, Sao Paulo, 14.040-904, Brazil
Tel) 55-16-3315-3953, E-mail) hugo.gaeta@usp.br

peri-implant bone loss and specific structures may not be visible on these radiographs.[9-11] Three-dimensional imaging modalities, such as cone-beam computed tomography (CBCT), offer better visualization through high-resolution images of the bone tissue in the peri-implant region.[9,12-15] CBCT can also diagnose peri-implant defects with sub-millimeter precision.[7] However, the presence of the implant generates metallic artifacts on CBCT.[16]

CBCT images may accurately and effectively display peri-implant deficiencies in the buccolingual plane.[11,14] This imaging modality can reveal dehiscence and fenestrations affecting the cortical bone around the implant.[11] However, the use of CBCT to assess particulate bone grafts used in the immediate implant technique is challenging, as these grafts appear as sparse high-density granules. Nevertheless, CBCT remains an essential tool for determining the success of implant treatment by confirming the filling of the spaces between bone tissue and the implant.[17] Notably, previous studies have not evaluated the accuracy of CBCT in assessing bone grafts near dental implants.

The aim of this study was to evaluate the effect of CBCT milliamperage (mA) on the detection of bone graft dehiscence around titanium and zirconia implants. The null hypothesis was that the type of implant and the mA level do not affect bone graft dehiscence detection adjacent to dental implants.

Materials and Methods

The study adheres to the standards published by the National Council for the Control of Animal Experimentation (CONCEA) and was approved by the Ethics Committee for Animal Research of the Federal University of Alfenas under protocol number 0018/2022 (CEUA: 3641cc56e4bf17852287b1fdba47a1e1).

The sample consisted of 40 bone blocks with approximate dimensions of 4 cm × 4 cm × 2 cm, obtained from fresh bovine ribs.[18,19] Only blocks with an appropriate thickness for simulating the gap around the implant and a balanced ratio of cortical and trabecular bone tissue were included (Fig. 1A).

A Ø8-mm trephine bur (WF Cirúrgicos Ltda., São Paulo, SP, Brazil) was used to drill a bone defect with a depth of 5 mm, ensuring at least a 2-mm gap between the implant and the bone block on all faces (Fig. 1B). For autogenous bone graft collection, a trephine drill was employed to extract bone from the bovine rib (Fig. 1C).

For 20 of the bone blocks, in the center of the bone defect (Fig. 1D), a titanium implant (Neodent CM Drive Acqua; Neodent, Curitiba, PR, Brazil) measuring 3.5 mm in diameter by 10 mm in length was inserted (Fig. 1E) by an experienced specialist in implantodontics. For the remaining 20 blocks, a zirconia implant (Neodent Zirconia; Neodent) measuring 3.75 mm in diameter by 10 mm in length

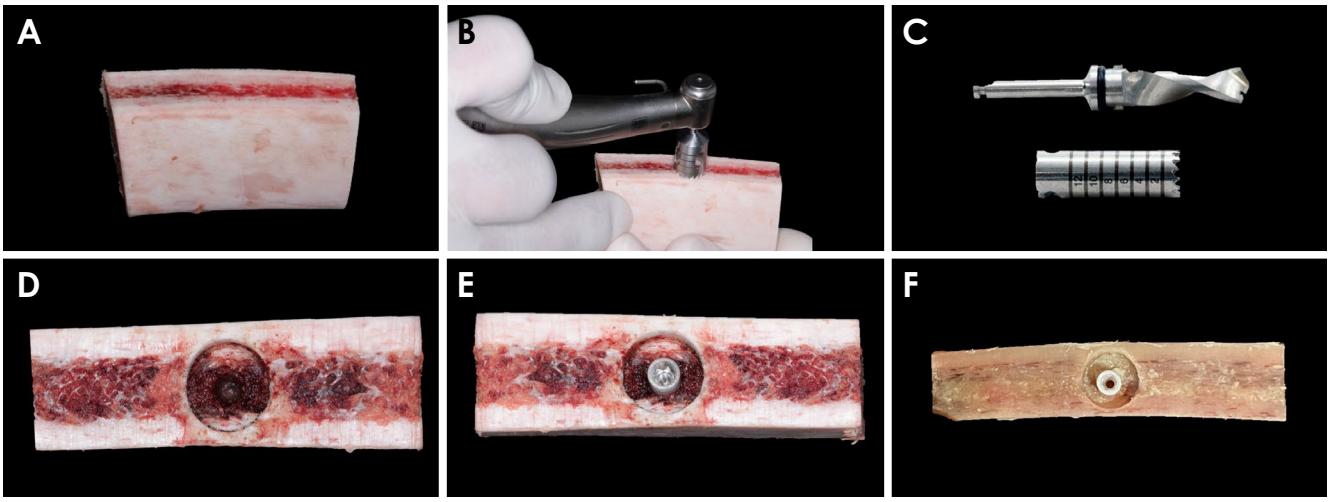

Fig. 1. A. Bone blocks obtained from fresh bovine ribs, sectioned to approximate dimensions of 4 cm × 4 cm × 2 cm. B. A Ø8-mm trephine bur (WF Cirúrgicos Ltda., São Paulo, SP, Brazil) used to drill a bone defect 5 mm deep. C. A collector trephine bur employed to harvest bone tissue for bone graft simulation. D. A bone block after preparation for implant installation, with a gap between the cortical bone and the implant's planned position in the center of the defect. E. A titanium implant (Neodent CM Drive Acqua; Neodent, Curitiba, PR, Brazil) measuring 3.5 mm in diameter and 10 mm in length placed on a bone block. F. A zirconia implant (Neodent Zirconia; Neodent) measuring 3.75 mm in diameter and 10 mm in length placed on a bone block.

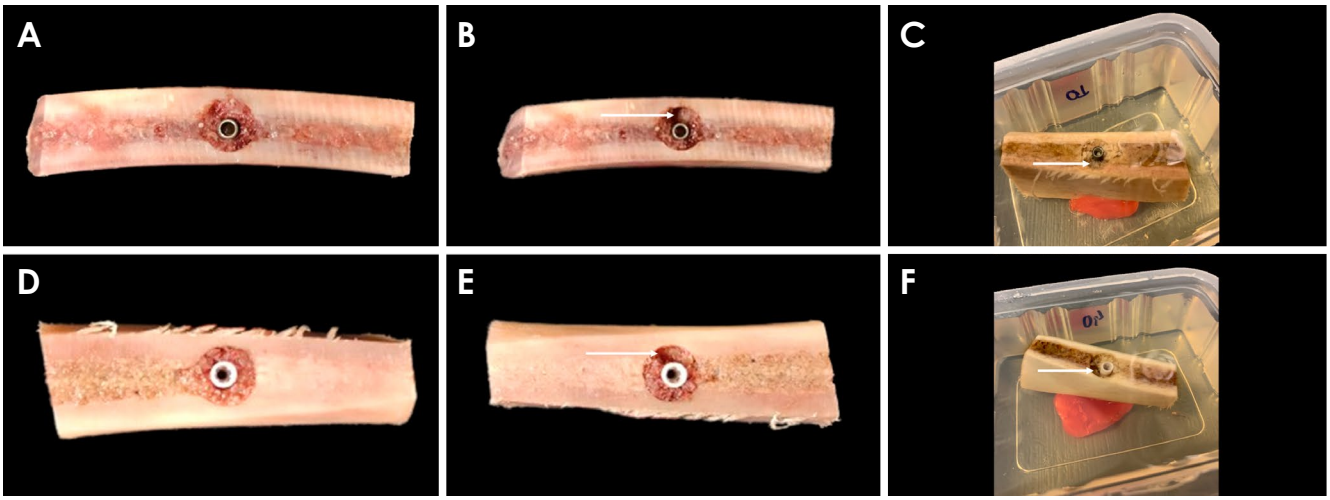

Fig. 2. A. Bone block with a titanium implant, with the gap between the implant and the cortical bone completely filled with bone graft. B. The arrow indicates the simulation of bone graft dehiscence; the bone graft was removed up to the third implant thread. C. Bone block placed individually in a plastic container and covered with ballistic gelatin to simulate soft tissue. D. Bone block with a zirconia implant, with the gap between the implant and the cortical bone completely filled with bone graft. E. Arrow indicates the simulation of bone graft dehiscence; the bone graft was removed up to the third implant thread. F. Bone block placed individually in a plastic container and covered with ballistic gelatin to simulate soft tissue.

was inserted into the center of the defect (Fig. 1F). The process was performed using an implant motor (NSK Surgic Pro; NSK Ltd., Kanuma, Tochigi, Japan) and a surgical contra-angle handpiece (Ti-Max X-SG20L; NSK Ltd.). Implant placement was carried out according to the manufacturers' specifications.

The acquired bone graft material was carefully positioned around the implant site to fill the entire gap (Figs. 2A and D). To establish a bone defect, the autogenous bone graft material was removed from the vestibular area of 10 titanium implants and 10 zirconia implants up to the third thread (Figs. 2B and E).

The prepared bone blocks were placed individually in plastic containers and covered with ballistic gelatin to simulate soft tissue (Figs. 2C and F). The ballistic gelatin was prepared using 48 g of colorless gelatin (Royal; Hypera Pharma, Jundiaí, SP, Brazil), 200 mL of distilled glycerin (Razzo; Razzo Ltda., São Paulo, SP, Brazil), and 500 mL of water.[20] The ballistic gelatin surrounded the bone blocks with the implants installed and was kept refrigerated until image acquisition.

CBCT images of the specimens were acquired using an OP300 system (Instrumentarium Dental, Tuusula, Finland) following a fixed protocol with a kilovoltage (kV) of 90 kV, a field of view (FOV) of 6 cm × 4 cm, a voxel size of 0.133 mm, and 3 different mA levels (4, 6.3, and 10 mA), resulting in a total of 120 volumes. To ensure consistent positioning of the specimens across all acquisitions, a polystyrene platform and a permanent marker were used, and reference lights were employed to standardize the placement of the bone blocks in the center of the FOV. Images were acquired for all implant groups, for both the gaps filled with bone graft and those with bone graft removed up to the implant's third thread (Fig. 3).

Images were exported from the acquisition software in Digital Imaging and Communications in Medicine (DICOM) format. Five evaluators (4 oral radiologists and 1 experienced specialist in implantodontics), each with a minimum of 5 years of experience in CBCT image evaluation, underwent a comprehensive training session during which the condition being assessed (peri-implant bone graft dehiscence) was explained. Evaluation sessions were held in a controlled environment with reduced ambient lighting conducive to CBCT image assessment. The evaluators used high-performance monitors (MDRC-2222; Barco, Kortrijk, Belgium) and OnDemand 3D version 1.0 (Cybermed Inc., Seoul, Korea). The original volumes of each exam were available, allowing the evaluators to perform a dynamic assessment through axial, coronal, sagittal, and cross-sectional reconstructions. The slice thickness was set to the minimum, corresponding to the voxel size (0.133 mm).

For each exam, the evaluators were required to dynamically assess the volume (i.e., scroll through the slices), adjust the window/level if necessary, and assign a score for the presence of bone graft dehiscence according to a 5-point scale, described as follows: 1, certainly no bone

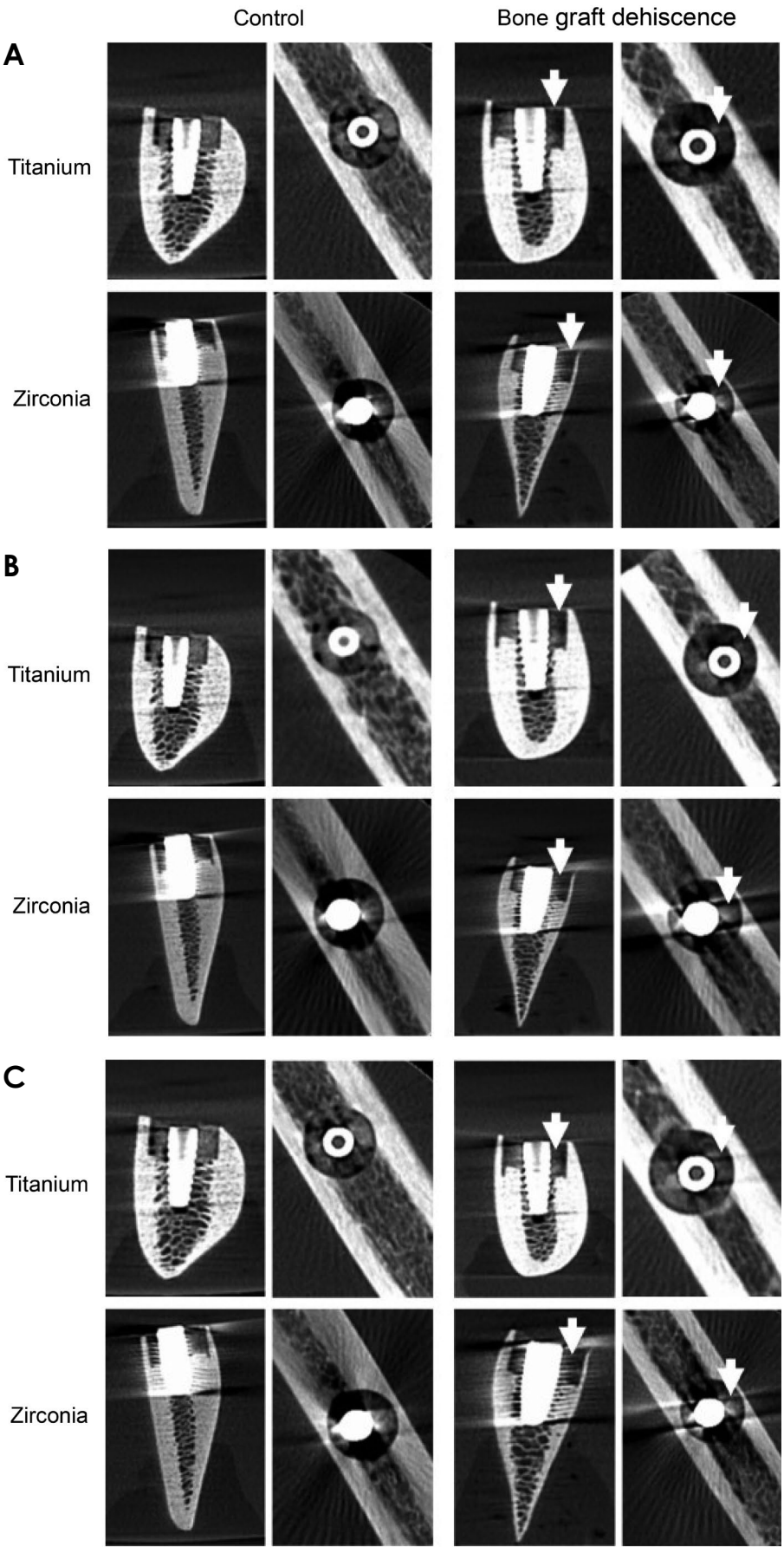

Fig. 3. Images acquired at 4 mA (A), 6.3 mA (B), and 10 mA (C). In the rows, sagittal and axial views compare control and bone graft dehiscence conditions within the same implant type (titanium or zirconia). In the columns, these conditions are compared between implant types. Arrows indicate areas of bone graft dehiscence.

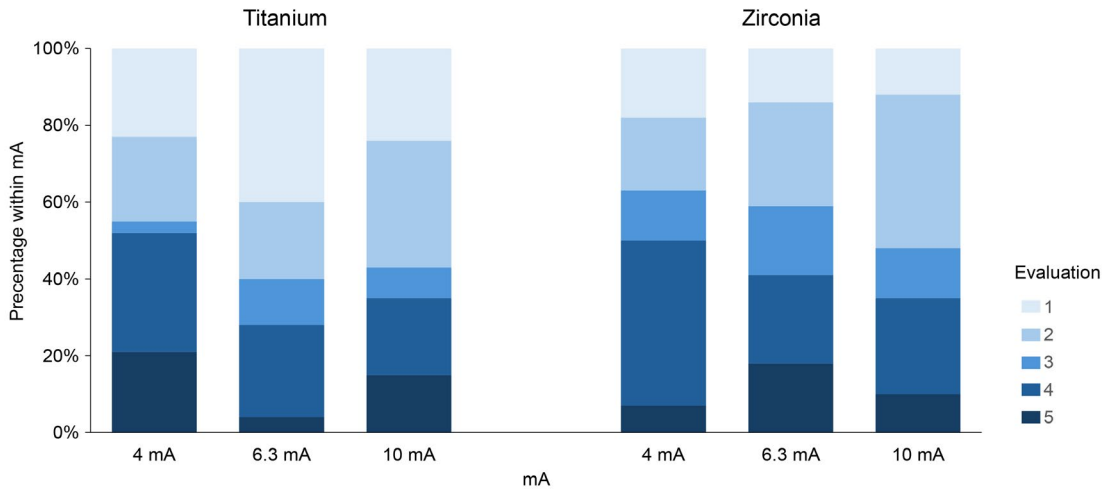

Fig. 4. Frequencies of scores, shown as percentages, across different implant materials and mA levels.

Table 1. Area under the receiver operating characteristic curve (AUC), accuracy, sensitivity, and specificity for detecting the presence of bone graft around titanium and zirconia implants at different milliamperage (mA) levels

	Titanium			Zirconia		
	4 mA	6.3 mA	10 mA	4 mA	6.3 mA	10 mA
AUC	0.78 ± 0.06	0.75 ± 0.12	0.65 ± 0.16	0.73 ± 0.07	0.85 ± 0.07	0.70 ± 0.11
Accuracy	0.67 ± 0.10	0.65 ± 0.14	0.63 ± 0.14	0.71 ± 0.04	0.69 ± 0.10	0.62 ± 0.08
Sensitivity	0.72 ± 0.16	0.70 ± 0.12	0.56 ± 0.23	0.84 ± 0.13	0.78 ± 0.24	0.60 ± 0.12
Specificity	0.62 ± 0.33	0.60 ± 0.38	0.70 ± 0.26	0.58 ± 0.16	0.60 ± 0.20	0.64 ± 0.11

graft dehiscence; 2, probably no bone graft dehiscence; 3, uncertain; 4, probably bone graft dehiscence; and 5, certainly bone graft dehiscence. The evaluators were instructed to assess 20 CBCT volumes per day to avoid visual fatigue and potential bias related to sample memorization. To assess the reproducibility of the image evaluation method, 25% of the sample was reevaluated after 30 days under the same conditions.

All data were analyzed using SPSS version 25.0 (IBM Corp., Armonk, NY, USA) and GraphPad Prism version 8 (GraphPad Software, San Diego, CA, USA). Intra-observer and inter-observer agreement were evaluated using the weighted kappa test for diagnostic evaluation. The frequency of each score was recorded based on the implant type and mA level and descriptively analyzed. Based on the 5-point scale evaluation, the area under the receiver operating characteristic curve (AUC) was calculated for the different mA and implant types. Additionally, diagnostic accuracy, sensitivity, and specificity values were calculated after data dichotomization, considering scores 1, 2, and 3 as indicating the absence of bone graft dehiscence and scores 4 and 5 as denoting its presence. These values were also calculated for the various mA levels and implant types. The diagnostic values were expressed as the mean and standard deviation (SD) among the evaluators for each condition - mA and implant type - and were compared using 2-way analysis of variance with a significance level of 5%.

Results

The mean intra-observer agreement was 0.726 (SD, 0.078; range, 0.600-0.792), indicating substantial agreement, while the mean inter-observer agreement was 0.193 (SD, 0.167; range, 0.082-0.662), indicating slight agreement.[21,22] In the evaluation of titanium implants, the score of 3 (uncertain) was relatively infrequent, occurring in 3% to 8% of cases across the different mA values. This implies that the evaluators were generally certain in their assessments. In comparison, the assessments of zirconia implants displayed higher frequencies of scores 2, 3, and 4 (probably no bone graft dehiscence, uncertain, and probably bone graft dehiscence, respectively). These ranged from 13% to

Table 2. Sum of sensitivity and specificity for titanium and zirconia implants at different milliamperage (mA) levels

Implant material	4 mA	6.3 mA	10 mA
Titanium	1.34	1.30	1.26
Zirconia	1.42	1.36	1.24

43%, suggesting greater uncertainty in the evaluations (Fig. 4).

Regarding the diagnosis of bone graft dehiscence, the AUC results indicated no statistically significant differences between implant types or mA levels ($P>0.05$) (Table 1). According to the evaluation scale developed by Hosmer et al. (2013),[23] all identified AUC values were within the acceptable range for diagnostic performance.

Similarly, no significant differences were observed in accuracy, sensitivity, or specificity ($P>0.05$, Table 1). According to Power et al.,[24] an examination must have a combined sensitivity and specificity of at least 1.5 to accurately predict the presence or absence of a disease. For both titanium and zirconia implants, all tests conducted at the different mA levels resulted in a combined sensitivity and specificity of less than 1.5 (Table 2), indicating that CBCT imaging does not achieve the desired diagnostic performance in assessing the presence or absence of bone graft dehiscence.

Discussion

The present study investigated the influence of different mA settings in CBCT exams on the detection of bone graft dehiscence around zirconia and titanium implants. The results did not display significant differences in detecting bone graft dehiscence, thus supporting the null hypothesis. Nevertheless, caution should be exercised when evaluating CBCT images for these diagnostic purposes, as the diagnostic values were somewhat low. Further research on dental implants and imaging exams is encouraged to advance diagnosis and treatment.

Initially, concerns were raised that zirconia implants might impede the identification of bone graft dehiscence, due to their higher atomic number relative to titanium and their greater potential to generate image artifacts. However, the results suggest no significant differences in detecting bone graft dehiscence around titanium or zirconia implants. These findings are consistent with those of Fontenele et al.,[25] who evaluated the detection of peri-implant dehiscence in titanium-zirconia and zirconia implants using CBCT images and found no significant differences between the implant types.

The use of a higher mA level improves image quality by reducing noise; however, the present results did not indicate significant differences among the mA settings used. Considering the correlation between mA and patient dose, this research suggests that it is possible to lower mA when evaluating bone grafts around titanium and zirconia implants without compromising diagnostic image quality. Pauwels et al.[26] investigated the impact of mA reduction on image quality with various CBCT devices to determine minimally acceptable values, employing a polymethyl methacrylate and an anthropomorphic skull phantom. This research revealed that mA can be reduced to lower patient dose with minimal impact on image quality, a promising finding that aligns with our results.

Although CBCT device manufacturers define image acquisition protocols, decreasing mA and limiting radiation exposure did not appear to substantially impact diagnostic accuracy. Nevertheless, other acquisition and reconstruction parameters influence image quality and radiation dose, which could affect diagnostic performance. Thus, it is reasonable to propose the existence of an exposure threshold, beyond which substantial differences between titanium and zirconia implants may emerge. In this context, Chang et al.[27] conducted a study to identify xenogenous bone graft dehiscence around different implant types using CBCT images with metal artifact reduction algorithms. Using the OP300 device (as in the present study), they observed lower diagnostic values for zirconia implants compared to titanium without the algorithm, whereas with the algorithm, no significant difference was found between these types.

Although reducing mA can lower patient radiation exposure, the present results showed only slight to moderate inter-observer agreement, suggesting that the diagnostic task is challenging. This contrasts with Pauwels et al.,[26] who demonstrated that minimally acceptable mA settings can effectively achieve high inter-observer agreement when evaluating anatomical structures in phantoms. Nevertheless, the differences in the inter-rater agreement likely relate to the nature of the task, as detecting well-defined anatomical structures is easier than detecting sparse graft material, especially in the presence of image artifacts. This complexity is reflected in the observed agreement values, which ranged from slight (0.01-0.20) to moderate (0.41-0.60) agreement. Notably, these values were calculated using the weighted kappa statistic, which can vary between -1 and $+1$; a positive value indicates that the observed agreement is greater than expected by chance[28] and thus re-

liable.

In this study, substantial intra-observer agreement was observed. This supports the reliability of the raters' analyses, as they remained consistent upon reanalysis of the imaging exams. Other studies in the literature have reported high intra-observer agreement in assessing bone grafts, as demonstrated by Parsa et al.,[29] who similarly evaluated the accuracy of CBCT in detecting bone grafts in an ex vivo study, and by Umanjec-Korac et al.,[30] who assessed the detection of simulated autogenous bone graft resorption in the maxillary sinus using CBCT.

This *ex vivo* study has inherent limitations in its design. Importantly, the methodology employed is the only ethically acceptable way to assess peri-implant dehiscence and factors such as implant material and mA level using repeated CBCT scans, as it would be unethical to expose a patient to repeated imaging acquisitions. Bovine ribs were used to simulate the anatomy of the human mandible in CBCT images due to their structural similarity, as demonstrated in research by Dave et al.[31] Autogenous bone grafts were also used, sourced from the same bovine ribs. However, the tomographic density of these bone grafts makes them challenging to visualize, as evidenced by the low inter-observer agreement. These obstacles are consistent with prior findings in the literature; for instance, Fienitz et al.[7] assessed the accuracy of CBCT in evaluating peri-implant bone defect regeneration after bone grafting and found difficulties in distinguishing between the bone graft and native bone. In contrast, our results differ from those of Bucchi et al.,[32] who did not encounter problems in detecting synthetic bone grafts throughout the healing process. However, synthetic bone grafts appear to have higher tomographic density, which could make them easier to detect compared to native bone grafts. Therefore, these limitations should be considered when interpreting and generalizing the conclusions of this study.

The present study aimed to improve the clinical significance of CBCT by applying the ALADA ("as low as diagnostically achievable") principle.[33] The use of low mA values meaningfully reduces patients' radiation exposure without compromising diagnostic quality. Minimizing radiation exposure during the diagnostic process prioritizes patient well-being by mitigating the risks associated with excessive ionizing radiation. However, bone grafts near implants can be difficult to visualize due to their discreet appearance and imaging artifacts caused by the high density of titanium and zirconia. In accordance with radiation protection guidelines, this study supports the use of CBCT protocols with low mA settings to assess bone grafts around dental implants, provided that the images are analyzed with caution.

In conclusion, low-mA CBCT protocols can be used to assess bone graft dehiscence near titanium and zirconia implants. However, caution is warranted when using CBCT to evaluate bone graft dehiscence adjacent to different implant types due to factors such as imaging artifacts caused by the implants, which can lead to misdiagnosis.

Conflicts of Interest: None

References

1. Bassir SH, El Kholy K, Chen CY, Lee KH, Intini G. Outcome of early dental implant placement versus other dental implant placement protocols: a systematic review and meta-analysis. J Periodontol 2019; 90: 493-506.
2. Ragucci GM, Elnayef B, Criado-Cámara E, Del Amo FS, Hernández-Alfaro F. Immediate implant placement in molar extraction sockets: a systematic review and meta-analysis. Int J Implant Dent 2020; 6: 40.
3. Araújo MG, Wennström JL, Lindhe J. Modeling of the buccal and lingual bone walls of fresh extraction sites following implant installation. Clin Oral Implants Res 2006; 17: 606-14.
4. Cardaropoli D, Tamagnone L, Roffredo A, De Maria A, Gaveglio L. Preservation of peri-implant hard tissues following immediate postextraction implant placement. Part I: radiologic evaluation. Int J Periodontics Restorative Dent 2019; 39: 633-41.
5. Ribeiro M, Fraguas EH, Brito KI, Kim YJ, Pallos D, Sendyk WR. Bone autografts & allografts placed simultaneously with dental implants in rabbits. J Craniomaxillofac Surg 2018; 46: 142-7.
6. AlKudmani H, Al Jasser R, Andreana S. Is bone graft or guided bone regeneration needed when placing immediate dental implants? a systematic review. Implant Dent 2017; 26: 936-44.
7. Fienitz T, Schwarz F, Ritter L, Dreiseidler T, Becker J, Rothamel D. Accuracy of cone beam computed tomography in assessing peri-implant bone defect regeneration: a histologically controlled study in dogs. Clin Oral Implants Res 2012; 23: 882-7.
8. Mengel R, Kruse B, Flores-de-Jacoby L. Digital volume tomography in the diagnosis of peri-implant defects: an in vitro study on native pig mandibles. J Periodontol 2006; 77: 1234-41.
9. Bohner LO, Mukai E, Oderich E, Porporatti AL, Pacheco-Pereira C, Tortamano P, et al. Comparative analysis of imaging techniques for diagnostic accuracy of peri-implant bone defects: a meta-analysis. Oral Surg Oral Med Oral Pathol Oral Radiol 2017; 124: 432-40.e5.
10. Jacobs R, Vranckx M, Vanderstuyft T, Quirynen M, Salmon B. CBCT vs other imaging modalities to assess peri-implant bone and diagnose complications: a systematic review. Eur J Oral Implantol. 2018; 11 Suppl 1: 77-92.

11. Pelekos G, Acharya A, Tonetti MS, Bornstein MM. Diagnostic performance of cone beam computed tomography in assessing peri-implant bone loss: a systematic review. Clin Oral Implants Res 2018; 29: 443-64.
12. Benic GI, Elmasry M, Hämmerle CH. Novel digital imaging techniques to assess the outcome in oral rehabilitation with dental implants: a narrative review. Clin Oral Implants Res 2015; 26 Suppl 1: 86-96.
13. Mol A. Imaging methods in periodontology. Periodontol 2000 2004; 34: 34-48.
14. Yepes JF, Al-Sabbagh M. Use of cone-beam computed tomography in early detection of implant failure. Dent Clin North Am 2015; 59: 41-56.
15. Wang D, Künzel A, Golubovic V, Mihatovic I, John G, Chen Z, et al. Accuracy of peri-implant bone thickness and validity of assessing bone augmentation material using cone beam computed tomography. Clin Oral Investig 2013; 17: 1601-9.
16. Kurt MH, Bağış N, Evli C, Atakan C, Orhan K. Comparison of the different voxel sizes in the estimation of peri-implant fenestration defects using cone beam computed tomography: an ex vivo study. Int J Implant Dent 2020; 6: 58.
17. Ritter L, Elger MC, Rothamel D, Fienitz T, Zinser M, Schwarz F, et al. Accuracy of peri-implant bone evaluation using cone beam CT, digital intra-oral radiographs and histology. Dentomaxillofac Radiol 2014; 43: 20130088.
18. Pinheiro LR, Gaia BF, Oliveira de Sales MA, Umetsubo OS, Santos Junior O, Cavalcanti MG. Effect of field of view in the detection of chemically created peri-implant bone defects in bovine ribs using cone beam computed tomography: an in vitro study. Oral Surg Oral Med Oral Pathol Oral Radiol 2015; 120: 69-77.
19. Vidor MM, Liedke GS, Vizzotto MB, da Silveira PF, da Silveira HL, Araujo CW, et al. Imaging evaluating of the implant/bone interface - an in vitro radiographic study. Dentomaxillofac Radiol 2017; 46: 20160296.
20. Nascimento EH, Fontenele RC, Santaella GM, Freitas DQ. Difference in the artefacts production and the performance of the metal artefact reduction (MAR) tool between the buccal and lingual cortical plates adjacent to zirconium dental implant. Dentomaxillofac Radiol. 2019; 48: 20190058.
21. Landis JR, Koch GG. The measurement of observer agreement for categorical data. Biometrics 1977; 33: 159-74.
22. Viera AJ, Garrett JM. Understanding interobserver agreement: the kappa statistic. Fam Med 2005; 37: 360-3.
23. Hosmer DW Jr, Lemeshow S, Sturdivant RX. Applied logistic regression. 3rd ed. Wiley; Hoboken: 2013. p. 500.
24. Power M, Fell G, Wright M. Principles for high-quality, high-value testing. Evid Based Med 2013; 18: 5-10.
25. Fontenele RC, Farias Gomes A, Nejaim Y, Freitas DQ. Do the tube current and metal artifact reduction influence the diagnosis of vertical root fracture in a tooth positioned in the vicinity of a zirconium implant? A CBCT study. Clin Oral Investig 2021; 25: 2229-35.
26. Pauwels R, Seynaeve L, Henriques JC, de Oliveira-Santos C, Souza PC, Westphalen FH, et al. Optimization of dental CBCT exposures through mAs reduction. Dentomaxillofac Radiol 2015; 44: 20150108.
27. Chang M, Felizardo HMA, Oliveira-Santos C, Gaêta-Araujo H. Influence of metal artifact reduction tool of two cone beam CT on the detection of bone graft loss around titanium and zirconium implants - an ex vivo diagnostic accuracy study. Clin Oral Implants Res (in press).
28. Gisev N, Bell JS, Chen TF. Interrater agreement and interrater reliability: key concepts, approaches, and applications. Res Social Adm Pharm 2013; 9: 330-8.
29. Parsa A, Ibrahim N, Hassan B, van der Stelt P, Wismeijer D. Bone quality evaluation at dental implant site using multislice CT, micro-CT, and cone beam CT. Clin Oral Implants Res 2015; 26: e1-7.
30. Umanjec-Korac S, Parsa A, Darvishan Nikoozad A, Wismeijer D, Hassan B. Accuracy of cone beam computed tomography in following simulated autogenous graft resorption in maxillary sinus augmentation procedure: an ex vivo study. Dentomaxillofac Radiol 2016; 45: 20160092.
31. Dave M, Davies J, Wilson R, Palmer R. A comparison of cone beam computed tomography and conventional periapical radiography at detecting peri-implant bone defects. Clin Oral Implants Res 2013; 24: 671-8.
32. Bucchi C, Borie E, Arias A, Dias FJ, Fuentes R. Radiopacity of alloplastic bone grafts measured with cone beam computed tomography: an analysis in rabbit calvaria. Bosn J Basic Med Sci 2017; 17: 61-6.
33. Jaju PP, Jaju SP. Cone-beam computed tomography: time to move from ALARA to ALADA. Imaging Sci Dent 2015; 45: 263-5.